University of Massachusetts Amherst

ScholarWorks@UMass Amherst

2010

Smooth Cascade of Wrinkles at the Edge of a Floating Elastic Film

J Huang
University of Massachusetts - Amherst

B Davidovitch
University of Massachusetts - Amherst, bdavidov@physics.umass.edu

C Santangelo
University of Massachusetts - Amherst, csantang@physics.umass.edu

T Russell

N Menon
University of Massachusetts - Amherst, menon@physics.umass.edu

Follow this and additional works at: https://scholarworks.umass.edu/physics_faculty_pubs

Part of the Physics Commons

A smooth cascade of wrinkles at the edge of a floating elastic film

Jiangshui Huang[1,2], Benny Davidovitch[1], Christian Santangelo[1], Thomas P. Russell[2], and Narayanan Menon*[1]

[1]*Department of Physics, University of Massachusetts, Amherst, Massachusetts 01003 and*
[2]*Polymer Science and Engineering Department, University of Massachusetts, Amherst, Massachusetts 01003*

(Dated: January 19, 2009)

The mechanism by which a patterned state accommodates the breaking of translational symmetry by a phase boundary or a sample wall has been addressed in the context of Landau branching in type-I superconductors [1], refinement of magnetic domains [2], and compressed elastic sheets [3]. We explore this issue by studying an ultra-thin polymer sheet floating on the surface of a fluid, decorated with a pattern of parallel wrinkles. At the edge of the sheet, this corrugated profile meets the fluid meniscus. Rather than branching of wrinkles into generations of ever-smaller sharp folds [3], we discover a smooth cascade in which the coarse pattern in the bulk is matched to fine structure at the edge by the continuous introduction of discrete, higher wavenumber Fourier modes. The observed multiscale morphology is controlled by a dimensionless parameter that quantifies the relative strength of the edge forces and the rigidity of the bulk pattern.

When a thin rectangular sheet floating on the surface of a pool of liquid is compressed along two opposing edges, it forms a pattern of wrinkles parallel to these edges. Unlike the Euler buckling of an unsupported piece of a paper, where the largest possible wavelength is selected, the wrinkles form at a wavelength $\lambda \ll W$, the width of the rectangle in the direction of the compression. Two principles are essential to understanding the amplitude and wavelength of this pattern: first, a thin sheet can, to a first approximation, be treated as inextensible, so that the length of a line in the compression direction is preserved. Consequently, the wavelength and amplitude of the wrinkles are related. Second, the bending energy of the sheet favours long wavelengths (and therefore large amplitudes) whereas the gravitational energy of the liquid subphase favours small amplitudes (and hence small wavelengths). Thus, the wavelength is selected by a compromise [5] between the bending energy of the sheet and gravitational energy (or more generally, any mechanism by which the subphase resists distortion).

We show in Fig.1 a controlled experimental realisation of this situation with a polystyrene (PS) sheet of dimensions $W \times L = 3cm \times 2cm$, and thickness t floating on the surface of water, and initially experiencing an isotropic tension $\approx \gamma$, the liquid-vapour surface tension. As the sheet is compressed by a distance Δ (such that $\tilde{\Delta} \equiv \Delta/W \ll 1$), parallel wrinkles develop in the bulk. The one-dimensional pattern of wrinkles in the bulk of
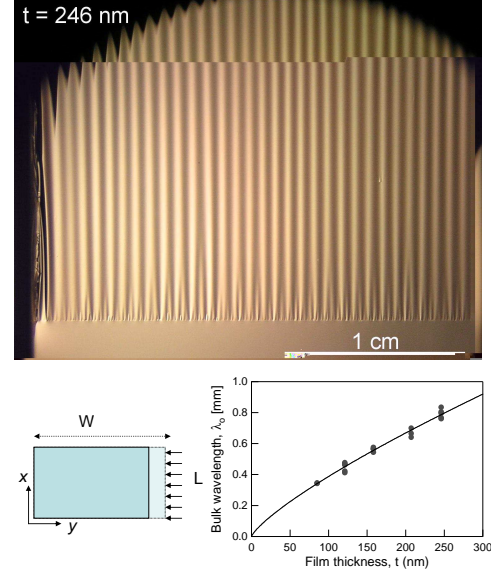

FIG. 1: (A) Image of a wrinkled PS sheet floating on the surface of water, compressed along its length between two razor blades. (B) Sketch of geometry. (C) Bulk wavelength of wrinkles, $\lambda = 2\pi/q_o$ as a function of film thickness, t. The solid line is a fit to $t^{3/4}$, showing agreement with the prediction of $q_o = (\rho g/B)^{1/4}$

the sheet, characterised by a height field $\zeta(y)$, has for small amplitudes, an energy per unit surface area:

$$u = \frac{1}{2}\Big(B(\frac{\partial^2\zeta}{\partial y^2})^2 + \rho g\zeta^2 + \sigma[(\frac{\partial\zeta}{\partial y})^2 - 2\tilde{\Delta}]\Big) \qquad (1)$$

The first two terms in $u(y)$ represent bending energy of the sheet and the gravitational energy of the fluid, respectively, while the third term enforces the constraint of inextensibility in the limit of small amplitudes, with the Lagrange multiplier σ being the stress σ_{yy} that must be applied in the y-direction at the compressed edges. ρ is the density of the fluid, and the bending modulus is denoted by $B = Et^3/(12(1 - \Lambda^2))$ [6], where E is the Young's modulus and Λ is the Poisson ratio. The surface tension does not appear in the energy functional shown above due to the fact that the bulk pattern has translational symmetry in the $\hat{x}$-direction. However, it is important to note that the sheet still experiences a tension $\sigma_{xx} \approx \gamma$. Minimising this energy density leads to a pattern

$$\zeta(y) = \frac{2}{q}\sqrt{\tilde{\Delta}}\sin(qy) \quad \textbf{(a)}; \; \sigma_{yy} = (Bq^2 + \rho g/q^2) \quad \textbf{(b)} \quad (2)$$

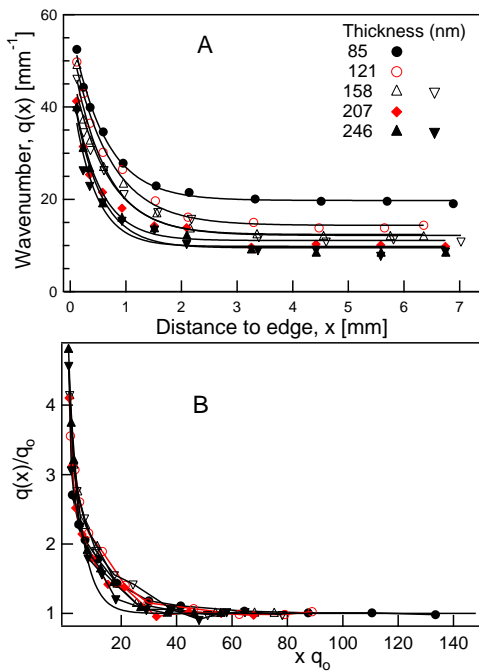where the wavenumber $q = q_o = (\rho g/B)^{1/4}$. With $q = q_o$,

FIG. 2: (A) Wavenumber $q(x)$ as a function of distance x from the edge of the sheet. The lengthscale over which the decay occurs does not change strongly with thickness t of the sheet. Exponential fits (solid lines) to $q(x)$ show systematic deviations but yield a decay length of $1.8 \pm 0.2mm$. By comparison, the capillary length $l_c = 2.7mm$ (B) Scaled wavenumber $q(x)/q_o$ versus the scaled distance from the edge xq_o. Data collapse is good at small and large xq_o, but there is poor collapse at intermediate distances indicating a multiscale evolution. The solid line shows an exponential fit.
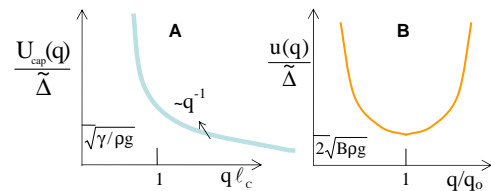

FIG. 3: (A) The energy per length of the meniscus, $U_{cap}(q_e) = 2\gamma(\tilde{\Delta}/q_e^2)\sqrt{(\rho g/\gamma) + q_e^2}$. (B) Energy per area of a sheet with wavenumber q, $u(q) = 2(\tilde{\Delta}/q^2)B(q^4 + q_o^4)$.

$\sigma_{yy} = -2\sqrt{B\rho g}$. As shown in Fig.1, this correctly describes the scaling of the wavelength of the wrinkles in the bulk. This scaling [5] has been experimentally tested [7, 8], and more broadly, applied in situations where the wavelength is determined by balancing the bending energy against substrate elasticity [9], capillary forces [10], and stretching under tensile forces [4].

However, in addition to the pattern in the bulk, inspection of Fig.1 shows a striking phenomenon: the parallel wrinkles of the bulk with wavenumber q_o, give way to a much finer structure of wrinkles near the uncompressed edge of the sheet. It is this cascade to ever-higher wavenumber that we examine in this Letter.

In Fig. 2A, we show for PS films of thickness t ranging from 85 to $246nm$, the increase in wavenumber $q(x)$ as a function of distance x from the uncompressed edge of the sheet. Since the bending modulus $B \sim t^3$, this represents a broad range of B. For all thicknesses, as the edge is approached, the wavenumber increases to a value at the edge q_e, that is 2-5 larger than the bulk value q_o. The evolution to higher wavenumbers occurs over approximately the same distance from the edge: though an exponential fit shows systematic deviations, such a fit estimates the penetration length of the edge into the bulk to be $1.8 \pm 0.2mm$.

Intuitively, a higher wavenumber at the edge is to be expected. The fluid meniscus follows the contour of the edge of the sheet. To minimise the surface energy of the air-water interface it is therefore favourable to reduce the amplitude of the wrinkles at the edge. In order to achieve this while preserving inextensibility, the wavenumber increases. This cascade to finer wrinkles must terminate at a finite wavenumber, q_e, where the gain in surface energy is offset by the increased energetic cost of bending. Notwithstanding these plausible arguments, previous experiments in this geometry [7] did not show a marked effect at the boundary of a film, and find that $q_e \approx q_o$. We thus need to address some obvious issues: What are the relevant parameters that dictate whether a cascade should be anticipated? When a cascade is observed, what governs the amplification of the bulk wavelength, and the length over which the cascade occurs?

In order to understand why wavenumber amplification occurs in our experiment, we estimate the energy cost of a wavenumber q_e at the edge. The capillary energy associated with the meniscus is $U_{cap} = 2\gamma(\tilde{\Delta}/q_e^2)\sqrt{(\rho g/\gamma) + q_e^2}$, which as sketched in Fig. 4A, is a decreasing function of q_e. To compare U_{cap}, which is an energy per unit length, to the energy cost per unit area of the affected part of the sheet (Fig. 4B), we require an understanding of the lengthscale over which the pattern at the edge penetrates into the sheet and matches the bulk pattern.

This leads us to consider the effect on the energy of the sheet of imposing a wavenumber q_e at its edge. The effect of broken translational symmetry in the $\hat{x}$-direction is incorporated by modifying Eq. 1 to:

$$u = \frac{1}{2}\Big(B(\nabla^2\zeta)^2 + \rho g\zeta^2 + \gamma(\frac{\partial\zeta}{\partial x})^2 + \sigma(x)[(\frac{\partial\zeta}{\partial y})^2 - 2\tilde{\Delta}]\Big). \quad (3)$$

The new, third, term, u_T quantifies the energy cost of the deformations in the $\hat{x}$-direction under the tension γ of the fluid tugging at the uncompressed edge of the sheet. When the compressive force in the y-direction is much smaller than the tensile force in the x-direction, $\varepsilon \equiv \gamma/\sigma = \gamma/\sqrt{\rho gB} \ll 1$, the minimal energy profile is determined by balancing bending and tensile forces [see Supplementary Information]. We thus develop a length scale, l_p, that will govern gradients in the x-direction. From $Bq_o^4 \sim \gamma l_p^{-2}$, we obtain $l_p \approx \sqrt{\gamma/\rho g}$, which is the

capillary length, l_c. This is consistent both with the magnitude of the typical penetration length found in Fig. 2, and with the insensitivity of this length scale to the thickness t. Furthermore, the stress ratio ε ranges between 6×10^{-4} and 3×10^{-3} in our experiments, thus validating the regime assumed in the foregoing argument.

A self-consistent argument for the strength of the wavelength amplification may be constructed by assuming that a single penetration length, l_p, governs the penetration of the edge wavenumber into the bulk; an estimate of the bending energy cost near the edge of the sheet is then obtained as $U_{edge} \sim l_p u(q_e) \sim B q_e^4 (\Delta/q_e^2)$. Setting the edge and meniscus energies to be comparable, $U_{edge} \sim U_{cap}$ we obtain $q_e \sim (\varepsilon)^{-1/3}\sqrt{(\gamma/B)}$. This argument shows that for $\epsilon \ll 1$ (as in our experiments) the wavenumber amplification is a large, nonperturbative effect on the bulk pattern. However, the estimate $U_{edge} \sim q_e^2$ derived above is wrong as it relies on the oversimplified picture of a single penetration length, unlike the cascade observed in Fig. 2 which indicates an elastic instability that leads to a symmetry-breaking sequence of period fissioning into intermediate wavenumbers (and correspondingly a sequence of penetration lengths). A full solution of the nonlinear problem [11] reveals that this instability results from a logarithmic dependence of $U_{edge} \sim \log q_e$, which lowers the energetic cost for sufficiently large values of q_e.

Assuming a pattern that is the superposition only of two wavenumbers q_0 and q_e, the penetration depth l_p exhibits a strong dependence on ϵ, ranging from l_c for $\epsilon \ll 1$ to q_0^{-1} for $\epsilon \gg 1$ (see Supplementary material). The latter limit, together with an energetic estimate similar to the one presented above, shows that for $\epsilon \gg 1$ the edge effect is only a small perturbation to the bulk pattern [7]. For $\epsilon \ll 1$ when there are wavenumbers q intermediate between q_0 and q_e, one can show that the length $l_p(q)$ of the transition zone between wavenumbers q and q_e, strongly depends on q, ranging from l_c for $q \to q_0$ to q_e^{-1} for $q \to q_e$. This is because a periodic wrinkling pattern with wave number $q > q_0$ requires enhancement of the compression $\sigma(x)$ towards the edge (thus increasing ϵ close to the edge). That the description in terms of a single penetration length l_p is simplified can be seen from Fig. 2B, where we show the scaled wavenumber $q(x)/q_0$ vs. the scaled distance from the edge xq_0. As anticipated, this scaling yields good data collapse far from the edge, and even close to the edge. However, data does not collapse in the intermediate region, indicating a wave-dependent penetration length $l_p(q)$.

Thus far, our estimates of the overall lengthscales of wavenumber amplification have shed no light on the nature of the cascade itself. The classic example of an elastic cascade was predicted by Pomeau and Rica [3] for the so-called "curtain geometry" of a tension-free sheet rippled under a compressive force but constrained to be flat at one edge. They showed that the matching of the
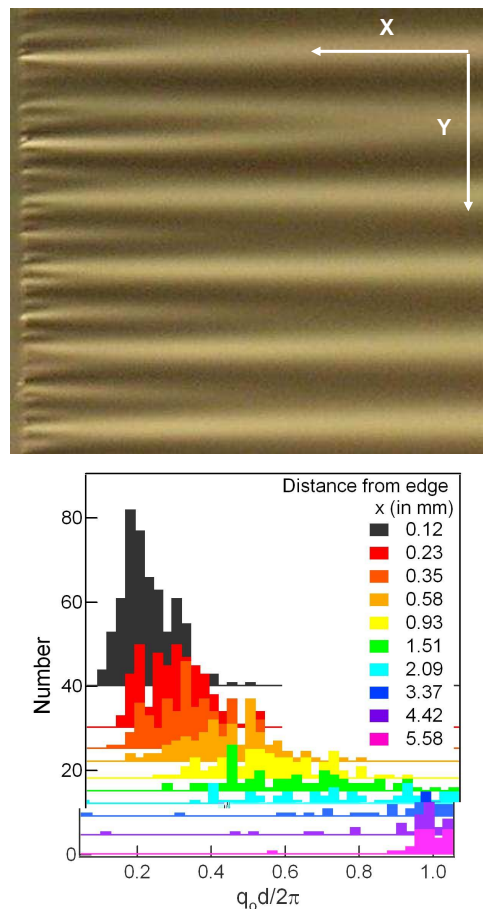

FIG. 4: (A) A magnified image of the cascade. (B) At each value of x, a histogram of the scaled separation, $q_o d/(2\pi)$, between crests, for several values of distance x from the edge. Data were collected from two films with $t = 246 nm$. The separations d, are determined from the locations of maxima of the intensity in the $\hat{y}$ direction.

ripples to the flat edge ($q_e \to \infty$) was achieved by an infinite hierarchy of branching events, in which each wrinkle branches into a succession of sharp folds with flat faces.

One superficial difference between what we observe and the Pomeau-Rica cascade is that our cascade terminates at a finite wavenumber, and therefore passes through only a few generations. The more profound difference stems from the fact that our sheets experience a tension along the uncompressed direction. Any deviation from a one-dimensional wrinkling pattern imposes curvature in both directions; this Gaussian curvature generates in-plane stretching energy controlled by a modulus $Y = Et$. In the tensionless Pomeau-Rica scenario, the dominant contribution to the strain energy is the anharmonic energy density $u_G \sim Y \zeta_x^2 \zeta_y^2$, whose minimisation leads to localised Gaussian curvature along a sequence of sharp ridges [12]. However, the consequence of the applied tension is that the focusing of Gaussian curvature does not fully relieve the strain energy at other points: as noted in Eq. 3, the tension term u_T penalises slope, and is non-zero even on flat facets where the gaussian curvature

vanishes. This mechanism thus favours a smooth reduction of the amplitude, which is naturally accomplished by the superposition of a finite number of Fourier modes with distinct wavenumbers. A transition between the Pomeau-Rica cascade and a smooth pattern is expected if $u_T \approx u_G$, which implies [see Supplementary Material] $\tilde{\Delta} < T/Y$. Together with the threshold condition for wrinkling $\tilde{\Delta} > \sigma_0/Y$ we see that a necessary condition for a smooth pattern is that the tension be large enough such that $\varepsilon \lesssim 1$. The characteristic values of ε in our experiments are well within this regime indicating a novel, smooth hierarchy, markedly different from the Pomeau-Rica stress-focusing cascade.

A closer look at the cascade, as shown in the magnified view of Fig. 4A, supports this new scenario of a smooth mechanism in which larger amplitudes of higher wavenumber Fourier components are smoothly mixed in as one approaches the edge. In Fig. 4B we present a more quantitative measure of the smoothness of the cascade. At a given distance x from the uncompressed edge we determine from the image, the separations d, between the crests of the wrinkles. At each value of x, we show a histogram of $q_o d/(2\pi)$, the normalised separation between wrinkles. Far away from the edge, the separations are all concentrated at $q_o d/(2\pi) = 1$. As expected, closer to the edge, more crests are formed, and at smaller values of d. Importantly, none of the histograms show significant weight near $d = 0$. In a scenario where wrinkles divide by localised branching, one might expect a preponderance of small values of d just after a branch-point, between sibling branches of the same parent wrinkle. That appears not to be the case in Fig. 4, with separations flowing smoothly to a mixture of higher Fourier components.

The three forces operative in this problem – gravity, bending energies, and surface energies – can be combined in pairs to yield three distinct length-scales: $(\rho g/B)^{1/4}$, $(\gamma/B)^{1/2}$ and $l_c = (\gamma/\rho g)^{1/2}$. The first of these is q_o, the second, an elastocapillary length [13] which controls q_e, and the third is the capillary length, which determines the length of the cascade. However, we emphasise that the stress ratio $\varepsilon = \sigma/\gamma$ dictates the overall morphology of the pattern in our experiments. Surface tension plays a dual role in our experiments, determining both the energy of the fluid meniscus, U_{cap}, as well as the tension applied in the uncompressed direction. In principle, these are different effects that could be independently tuned. Increasing the capillary energy cost of the edge can tune a transition from the regime of our experiment to that of stiffer sheets, in which the effect of the edge is small. On the other hand, decreasing the applied tension could drive a transition from the smooth, energy-delocalised cascades we observe, to a regime of localised branching [3] with energy-focusing. Thus, our observations open the way to the exploration of a rich phase diagram [11] of both branched and smooth structures.

Materials and Methods: The films were prepared from solutions of polystyrene (PS; atactic, number-average molecular weight $M_n = 121K$, weight-average molecular weight $M_w = 1.05M_n$, radius of gyration R_g $10nm$) in toluene, spin-coated on to glass substrates. The film thickness t was varied by changing the concentration of the solution and the spin rate, and was measured by x-ray reflectivity using a Panalytical X-Pert x-ray diffractometer. The $CuK\alpha$ radiation from the x-ray source (wavelength $\lambda = 0.154nm$) is coupled to a parabolic, graded multilayer mirror assembly that produces a low-divergence beam of x-rays incident on the PS film. Observation of the Kiessig fringes in specular reflection with a two-circle goniometer yielded the film t with a precision of $\pm0.5nm$.

A rectangle of dimensions $L \times W = 2cm \times 3cm$ was scribed onto the film with a sharp edge. When the substrate was dipped into a petri dish of distilled, deionized water, a rectangular piece of the PS film detached from the substrate. Because PS is hydrophobic, the film remained at the air-water interface. In order to prepare extremely well-defined edges, in a few selected cases, we spin-coated the film on a silicon wafer with an oxidised surface layer. Rather than scribing the film, the silicon substrate was fractured along a crystalline plane, and the PS film was lifted off with HF solution.

Author contributions Experiment design: JH, TPR, NM; Data: JH; Analysis: JH, NM with ideas developed with BD; Theory: BD, CS; Manuscript preparation: NM, BD with input from TPR, CS.

[1] R.P. Huebener, *Magnetic Flux Structures in Superconductors*, Springer 2001.

[2] A. Hubert, R. Schäfer, *Magnetic Domains: The Analysis of Magnetic Microstructures*, Springer, 1998

[3] Y.Pomeau and S.Rica, Plaques très comprimées, C.R. Acad. Sci. Paris., Ser.IIb **325**, 181 (1997).

[4] E.Cerda, K. Ravi-Chander, L.Mahadevan, Wrinkling of an elastic sheet under tension, Nature **419**, 579 (2002).

[5] E.Cerda and L.Mahadevan, Geometry and Physics of Wrinkling, Phys. Rev. Lett. **90**, 074302 (2003).

[6] L.D.Landau and L.M.Lifshitz, *Theory of Elasticity* (Pergamon,New York, 1986)

[7] L.Pocivavsek *et al.*, Stress and Fold Localization in Thin Elastic Membranes, Science **320**, 912 (2008).

[8] D. Vella, P. Aussillous, L. Mahadevan, Elasticity of an interfacial particle raft, Europhys. Lett., **68**, 212 (2004).

[9] C. M. Stafford et al., A buckling-based metrology for

measuring the elastic moduli of polymeric thin films Nature Mater., **3**, 545 (2004).

[10] J. Huang et al., Capillary Wrinkling of Thin Floating Polymer Films, Science **317**, 650 (2007).

[11] B. Davidovitch, manuscript.

[12] T.A.Witten, Stress focusing in elastic sheets, Rev. Mod. Phys. **79**, 643 (2007).

[13] J. Bico, B. Roman, L. Moulin, A. Boudaoud, Elastocapillary coalescence in wet hair, Nature, **432**, 690 (2004).